ChemComm

COMMUNICATION

View Article Online
View Journal | View Issue

Cite this: *Chem. Commun.*, 2016, 52, 5957

Received 29th February 2016,
Accepted 29th March 2016

DOI: 10.1039/c6cc01797e

www.rsc.org/chemcomm

A near-infrared AIEgen for specific imaging of lipid droplets†

Miaomiao Kang,‡[ab] Xinggui Gu,‡[ac] Ryan T. K. Kwok,[ac] Chris W. T. Leung,[ac] Jacky W. Y. Lam,[ac] Feng Li*[bd] and Ben Zhong Tang*[ace]

A new near-infrared AIE luminogen (TPE-AC) with high specificity, good biocompatibility and excellent photostability is designed and synthesized for lipid droplet (LD) imaging in cells. TPE-AC can monitor the process of LD accumulation in cells, thus making it potential for the diagnosis of early-stage fat-related diseases.

A liver is diagnosed as "fatty" when its hepatocytes contain more than 5% of triglycerides.[1,2] Fatty liver disease (FLD) acts as a worldwide hepatopathy threatening human health and is featured with the excessive accumulation of large lipid vesicles in liver cells *via* the process of steatosis.[3] Severe FLDs with extensive inflammation often lead to hepatitis. As liver is the primary organ of lipid metabolism,[4] methods involving computerized tomography scanning and B-type ultrasound have been developed and widely used for liver inspection and FLD diagnosis. These methods, however, suffer from poor sensitivity and can only be applied to the late-stage diagnosis of severe FLDs.[5] In order to recognize mild FLDs and other liver diseases at early stages, it still relies on transhepatic biopsy, which involves a invasive and risky procedure.[6] Thus, the development of new techniques that enable the direct and non-invasive detection of lipids in the liver would be of great medical importance.

As the storage sites of lipids in FLDs, detection of lipid droplets (LDs) has received increasing attention in biomedical science research.[7] LDs mainly locate in adipocytes, hepatocytes, adrenal cortex and myocytes,[8] and play important roles in regulating the storage and metabolism of neutral lipids, membrane formation and maintenance, signal transduction, protein degradation and so on.[9,10] The abnormality of LDs in cells is a critical biomarker for various diseases, such as FLD, hyperlipidaemia, type II diabetes and atherosclerosis.[11] Moreover, extensive literature reports that lipid peroxidation is closely correlated with neurodegeneration in Alzheimer's disease.[12,13] In addition, LDs in host cells are also associated with the pathogenesis of viruses and bacteria.[14] Much evidence shows that the unusual behaviour of LDs in cells should be considered as a crucial hallmark of cancers.[15] The development of new tools for monitoring the abnormal LD accumulation is thus of high importance, as it can provide useful information for the biomedical study and diagnosis of fat-related diseases at early stages.

Organic fluorophores have been widely used as visualizing agents in cell imaging owing to their intrinsic advantages of high sensitivity, good biocompatibility and direct observation.[16] Nile Red and BODIPY dyes are two kinds of commercial fluorophores for LD imaging.[17,18] However, they suffer from several disadvantages. For example, Nile Red exhibits poor selectivity to LDs as it stains other intracellular structures, leading to low image contrast.[19] BODIPY dyes, on the other hand, usually require long staining time and possess small Stokes' shifts.[20] Oil Red O is another LD-targeting dye but it can only stain fixed cells,[21] thus showing limited potential in dynamic monitoring of LDs in live cells. Apart from these, such conventional organic fluorophores also encounter the aggregation-caused quenching (ACQ) effect: their emissions are partially or completely quenched at high concentration or upon aggregate formation due to the generation of detrimental species like excimers and exciplexes by strong π–π* interactions.[22] Thus, they are often used at very

[a] *Department of Chemistry, Hong Kong Branch of Chinese National Engineering Research Center for Tissue Restoration & Reconstruction, Institute for Advanced Study, Division of Biomedical Engineering, Division of Life Science, State Key Laboratory of Molecular Neuroscience and Institute of Molecular Functional Materials, The Hong Kong University of Science and Technology, Clear Water Bay, Kowloon, Hong Kong, China. E-mail: tangbenz@ust.hk*

[b] *Department of Neurobiology and Anatomy, Zhongshan School of Medicine, Sun Yat-sen University, Guangzhou 510080, China. E-mail: lifeng@mail.sysu.edu.cn*

[c] *HKUST Shenzhen Research Institute, No. 9 Yuexing 1stRD, South Area, Hi-tech Park, Nanshan, Shenzhen 518057, China*

[d] *Guangdong Provincial Key Laboratory of Brain Function and Disease, Zhongshan School of Medicine, Sun Yat-sen University, Guangzhou 510080, China*

[e] *Guangdong Innovative Research Team, SCUT-HKUST Joint Research Laboratory, State Key Laboratory of Luminescent Materials and Devices, South China University of Technology, Guangzhou 510640, China*

† Electronic supplementary information (ESI) available: Detailed synthesis and characterization of TPE-AC and intermediates; absorption and PL spectra of TPE-AC powders; cytotoxicity of TPE-AC; particle size analysis; and fluorescence images of live and fixed cells stained with TPE-AC. See DOI: 10.1039/c6cc01797e

‡ M. K. and X. G. contributed equally to this work.

low concentrations, offering low photo-bleaching resistance, poor sensitivity and short retention time in cells.[23]

Aggregation-induced emission (AIE) is a process exactly opposite to the ACQ effect. Molecules with AIE features are generally non-emissive in solutions but are induced to emit by aggregate formation.[24–26] Owing to the high brightness and photostability of their aqueous nanosuspensions, AIE luminogens (AIEgens) have emerged as promising fluorescent stains for various biological applications.[24,27] As a result of the enthusiastic research effort in the past decade, a large variety of fluorescent probes with emission colours covering from blue to red have been developed and successfully applied in organelle-specific imaging such as mitochondria, plasma membranes and lysosomes.[23,28–31] However, only a few LD probes have been reported, and a representative example developed by us is TPE-AmAl.[32] Its aggregates have been found to selectively stain LDs with strong greenish blue light. To avoid the interference from autofluorescence of cells, it is more desirable to develop LD fluorescent probes with longer wavelength light excitation and emission. The absorption and emission of organic conjugated molecules are known to be tuned readily by introducing electron donors (D) and acceptors (A). In this regard, we have structurally modified TPE-AmAl and developed a new near-infrared (NIR) AIEgen, abbreviated as TPE-AC (Fig. 1), by decorating the tetraphenylethene (TPE) core with dimethylamine as the electron donor (D) and malononitrile as the electron acceptor (A). Due to the inheritance of the AIE feature from TPE, TPE-AC emits intensively in the aggregated state. Because of the stronger D–A interaction, TPE-AC absorbs and emits at a longer wavelength than TPE-AmAl. We also demonstrated that TPE-AC could stain LDs in both live and fixed cells with high specificity and good biocompatibility and photostability.

TPE-AC was synthesized by a two-step simple reaction route in a good yield (Scheme S1, ESI†). In brief, 1,2-bis(4-diethylaminophenyl)-1-(4-bromophenyl)-2-phenylethene (**1**) was first prepared according to our previous report.[32] Lithiation of **1** with *n*-BuLi followed by sequential acetylation with dimethylacetamide gave 1,2-bis(4-diethylaminophenyl)-1-(4-acetophenyl)-2-phenylethene (**2**) in a yield of 70%. TPE-AC was synthesized by the Knoevenagel condensation of **2** and malononitrile in a moderate yield of 50%. TPE-AC and the intermediates were characterized by NMR and mass spectroscopies, from which satisfactory results corresponding to their molecular structures were obtained (Fig. S1–S6, ESI†).

TPE-AC shows an absorption maximum at 455 nm in THF solution (Fig. 2A), which is red-shifted by ~45 nm compared to TPE-AmAl.[32] Such a red-shift is ascribed to the stronger

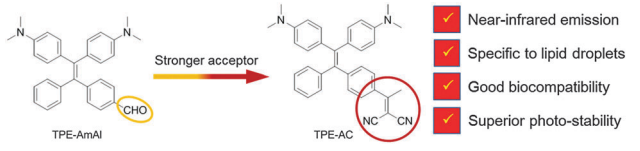

Fig. 1 Design rationale of a new near-infrared AIE luminogen for lipid droplet imaging.

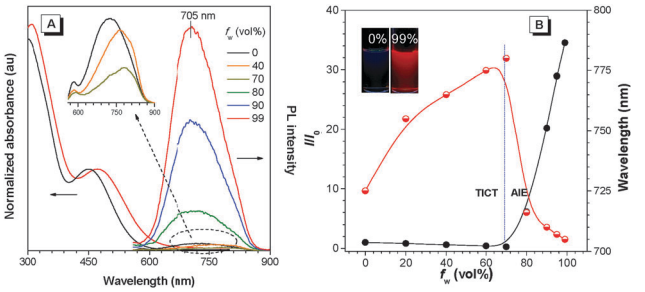

Fig. 2 (A) Absorption and PL spectra of TPE-AC in THF/water mixtures with different water fractions (f_w). Inset: Enlarged PL spectra at f_w of 0–70%. Concentration: 10 μM; λ_{ex} = 450 nm. (B) Plot of relative PL intensity (I/I_0) and emission maximum of TPE-AC *versus* the composition of the THF/water mixtures of TPE-AC, where I_0 is the PL intensity in THF solution. Inset: Photographs of TPE-AC in THF solution and THF/water mixture with 99% f_w taken under 365 nm UV light irradiation from a hand-held UV lamp. Concentration: 10 μM; λ_{ex} = 450 nm.

electron withdrawing effect of the malononitrile moiety in TPE-AC than the formyl group in TPE-AmAl, resulting in a stronger electron push–pull effect and a smaller energy gap for electronic transition. TPE-AC emits faintly in THF. Upon gradual addition of water, a poor solvent for the luminogen, from 0 to 70 vol% into its THF solution, the emission becomes weaker gradually and the emission maximum is continuously red-shifted from 724 to 780 nm (Fig. 2B). Such a phenomenon is attributed to the enhancement of the twisted intramolecular charge-transfer (TICT) effect from the electron donor to the acceptor of TPE-AC owing to the increment of the polarity of the solvent mixture upon water addition. At water fractions larger than 70%, TPE-AC is emissive again, possibly due to the formation of nanoaggregates of TPE-AC, which activates the AIE process. Such a claim is confirmed by dynamic light scattering analysis (Fig. S7, ESI†). At 99% water content, the PL intensity is about 34-fold higher than that in the pure THF solution. Clearly, TPE-AC is AIE-active. On the other hand, the increase in the hydrophobicity of the local environment of nanoaggregates results in a blue-shift in their emission. Although the extent of the blue-shift is small (20 nm), TPE-AC aggregates still show near-infrared emission at 705 nm with an absolute quantum yield of 5% (Fig. S8, ESI†). As bioimaging is always conducted in buffers or culture media, the emission properties of TPE-AC in the presence of phosphate buffered saline (PBS) is examined. As shown from the PL spectrum in Fig. S9 (ESI†), TPE-AC shows a similar response to PBS as water.

To explore the application of TPE-AC in LD imaging in live cells, its cytotoxicity was firstly evaluated using 3-(4,5-dimethyl-2-thiazolyl)-2,5-diphenyltetrazolium bromide (MTT) assay. As depicted in Fig. S10 (ESI†), no significant change in the cell viability is observed when the cells are cultured in the presence of a high concentration of TPE-AC of 100 μM for 24 h. This reveals that TPE-AC shows no cytotoxicity and good biocompatibility to live cells. The absorption and emission of TPE-AC in buffers with different pH values were then investigated. From the results shown in Fig. S11 (ESI†), the absorption and PL spectra change a little even when the pH value is varied from 4.06

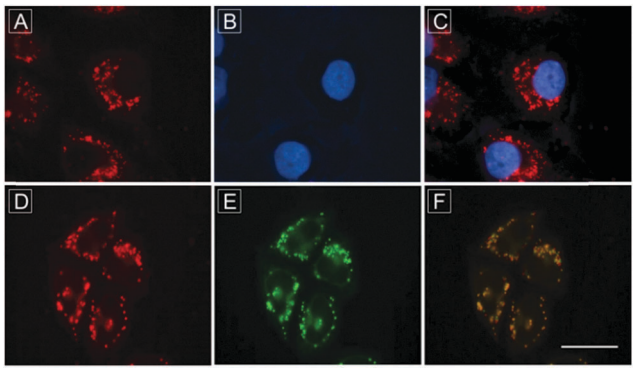

Fig. 3 (A and B) Fluorescence images of HeLa cells co-stained with (A) TPE-AC and (B) DAPI. (C) Merged image of (A) and (B). (D and E) Fluorescence images of HeLa cells co-stained with (D) TPE-AC and (E) BODIPY 493/503. (F) Merged image of (D) and (E). Concentration: 10 μM (TPE-AC), 1.5 μg mL^{-1} (DAPI) and 1 μg mL^{-1} (BODIPY 493/503); λ_{ex}: 510–550 nm (TPE-AC), 330–385 nm (DAPI), 460–490 nm (BODIPY 493/503); scale bar: 30 μm.

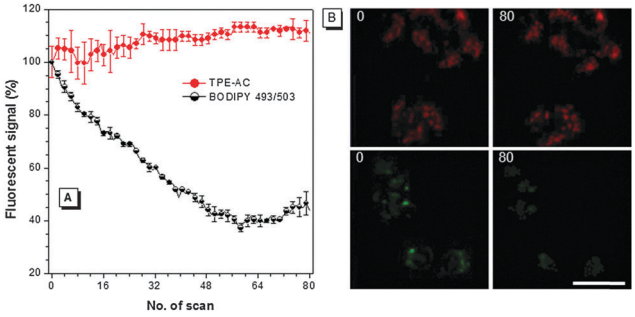

Fig. 4 (A) Loss in fluorescence of HeLa cells stained with TPE-AC and BODIPY 493/503 with the number of scans of laser irradiation. (B) Confocal images of HeLa cells stained with TPE-AC (upper panel) and BODIPY 493/503 (lower panel) before and after 80 scans of laser irradiation. Concentration: 10 μM (TPE-AC) and 1 μg mL^{-1} (BODIPY 493/503); λ_{ex}: 514 nm (TPE-AC) and 489 nm (BODIPY 493/503); laser power: 0.3 μW; scale bar: 40 μm.

to 9.20, indicating that TPE-AC is stable under physiological conditions.

We then investigated its capability to stain LDs in live cells by using a fluorescence microscope. HeLa cells were first treated with oleic acid, which is a fatty acid that can induce significant amounts of neutral lipids in cells,[7] and then co-stained with TPE-AC (10 μM) and a commercial nuclei-specific probe, namely DAPI (1.5 μg mL^{-1}). As shown from the fluorescence images of HeLa cells in Fig. 3A–C, red fluorescence from TPE-AC and blue fluorescence from DAPI are clearly observed in LDs and nucleus, respectively. It is of interest to note that TPE-AC emits a bright NIR light in LDs with high contrast even when the polarity of the local environment is low.[33]

In order to further assess the specificity of TPE-AC to LDs in live HeLa cells, BODIPY 493/503, a commercially available LDs-imaging agent, was used to co-stain the oleic acid-treated HeLa cells. The similarity between the fluorescence images shown in Fig. 3D and E suggests that both TPE-AC and BODIPY 493/503 stained the LDs in cells. The Pearson's correlation coefficient of the two fluorescence images is calculated to be 0.92, indicating that TPE-AC is highly specific to LDs. Interestingly, a clear image of LDs can be obtained with a considerable signal-to-noise ratio at a staining time as short as 15 min (Fig. S12A–D, ESI†). Furthermore, when the concentration of TPE-AC is increased to 100 μM, the staining process can be shortened to 2 min (Fig. S13, ESI†). These results suggest that TPE-AC can pass through the cell membrane easily and stain the LDs in a fast and convenient fashion.

To further examine whether TPE-AC only applies for HeLa cells we also used it to stain other cells, including LO2, LX2, HepG2 and MCF7 cells. As depicted in Fig. S14 (ESI†), after being treated with oleic acid and then stained with TPE-AC, all the cells show red emission from LDs. These results further support that TPE-AC is a universal fluorescent probe for LDs and is a potential material for various biological research studies.

Photostability is one of the key criteria for evaluating a fluorescent visualizer. To quantitatively investigate the photo-bleaching resistance of TPE-AC and BODIPY 493/503, we continuously scanned the dye-labelled HeLa cells with 0.3 μW laser excitations from a confocal fluorescence microscope, and recorded the corresponding fluorescence signal at each scan. The plot of percentage of signal loss against the scan number is shown in Fig. 4A. There was no significant signal loss in TPE-AC after 80 scans at a total irradiation time of 30 min.

In contrast, more than half of the fluorescence of BODIPY 493/503 is lost after 40 scans. The NIR fluorescence of TPE-AC can still be observed in LDs clearly after 80 scans, but the BODIPY emission almost disappears under the same conditions (Fig. 4B). Evidently, TPE-AC shows a much higher photostability than BODIPY 493/503.

Due to its advantages of bright NIR emission, low cytotoxicity, high specificity and excellent photostability in LD imaging, we further explored the application of TPE-AC in monitoring LD accumulation in cells. We treated the live cells with oleic acid for different incubation times and then used TPE-AC to stain the oleic acid-treated cells. Upon increasing the incubation time, more intense red fluorescence from HeLa cells was observed, indicating that more LDs are induced to be produced in the cytoplasm (Fig. 5A–D). We further studied the concentration effect of oleic acid on the amount of LDs. The HeLa cells were exposed to different oleic acid concentrations for 6 h followed by staining with TPE-AC. In the absence of oleic acid, only weak red fluorescence is observed (Fig. 5E). When the HeLa cells are treated at a higher acid concentration, a more intense PL signal is recorded, demonstrating that more LDs are visualized by TPE-AC (Fig. 5E–H). Thus, TPE-AC indeed can be used as a fluorescent probe to monitor the accumulation of LDs, making it potential for the early diagnosis of liver diseases.

In addition to fast staining and easy operation in live cell imaging, a versatile fluorescent probe should be capable of staining fixed cells as well because cell fixation is a critical step for sample preservation in biological research. As shown in Fig. S15 (ESI†), the specificity of TPE-AC to LDs remains high in fixed HeLa cells and COS-7 cells, demonstrating that it also works well in fixed samples.

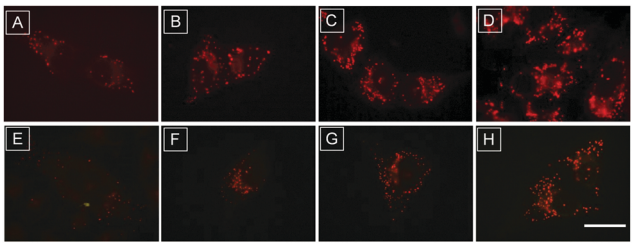

Fig. 5 (A–D) Fluorescence images of HeLa cells incubated with oleic acid (50 μM) for (A) 0.5 h, (B) 2 h, (C) 4 h, (D) 6 h, followed by staining with TPE-AC (10 μM). (E–H) Fluorescence images of HeLa cells incubated with (E) 0 μM, (F) 12.5 μM, (G) 25 μM and (H) 50 μM oleic acid for 6 h, followed by staining with TPE-AC (10 μM). λ_{ex}: 510–550 nm; scale bar: 30 μm.

In summary, in this work, a new NIR AIEgen is developed for specific LD imaging and monitoring LDs in live cells with high brightness, good biocompatibility and superior photostability. The long-wavelength absorption and emission of TPE-AC make it a promising material for *in vivo* deep tissue LD imaging, early diagnosis of liver diseases, and real-time monitoring of the macrophage foam cells.

This work was partially supported by the National Basic Research Program of China (973 Program, 2013CB834701 and 2013CB834702), the University Grants Committee of Hong Kong (AoE/P-03/08), the Innovation and Technology Commission (ITC-CNERC14S01), the Research Grants Council of Hong Kong (16301614, 16305015 and N_HKUST604/14), the Innovation and Technology Commission (ITC-CNERC14SC01), and the Guangdong Innovative Research Team Program (201101C0105067115). We thank the support from the National Natural Science Foundation of China (NSFC) Grant (81271476), Guangzhou Science and Technology Research Grant (201300000154) and the 111 Project Grant (B13037).

Notes and references

1 D. G. Tiniakos, M. B. Vos and E. M. Brunt, *Annu. Rev. Pathol.: Mech. Dis.*, 2010, **5**, 145.
2 D. E. Kleiner, E. M. Brunt, M. V. Natta, C. Behling, M. J. Contos, O. W. Cummings, L. D. Ferrell, Y. C. Liu, M. S. Torbenson, A. Unalp-Arida, M. Yeh, A. J. McCullough and A. J. Sanyal, *Hepatology*, 2005, **41**, 1313.
3 T. C. Walther and R. V. Farese, *Annu. Rev. Biochem.*, 2012, **81**, 687.
4 A. E. Crunk, J. Monks, A. Murakami, M. Jackman, P. S. Maclean, M. Ladinsky, E. S. Bales, S. Cain, D. J. Orlicky and J. L. McManaman, *PLoS One*, 2013, **8**, e67631.
5 T. Yonezawa, R. Kurata, M. Kimura and H. Inoko, *Mol. BioSyst.*, 2011, **7**, 91.
6 (*a*) R. Chapman, *Gut*, 2002, **51**, 9; (*b*) M. M. Skelly, P. D. James and S. D. Ryder, *J. Hepatol.*, 2001, **35**, 195.
7 Y. Fujimoto, J. Onoduka, K. J. Homma, S. Yamaguchi, M. Mori, Y. Higashi, M. Makita, T. Kinoshita, J. Noda, H. Itabe and T. Takanoa, *Biol. Pharm. Bull.*, 2006, **29**, 2174.
8 D. J. Murphy, *Prog. Lipid Res.*, 2001, **40**, 325.
9 (*a*) S. Martin and R. G. Parton, *Nat. Rev. Mol. Cell Biol.*, 2006, **7**, 373; (*b*) H. Zhang, Y. Wang, J. Li, J. Yu, J. Pu, L. Li, H. Zhang, S. Zhang, G. Peng, F. Yang and P. Liu, *J. Proteome Res.*, 2011, **10**, 4757.
10 A. W. Cohen, B. Razani, W. Schubert, T. M. Williams, X. B. Wang, P. Iyengar, D. L. Brasaemle, P. E. Scherer and M. P. Lisanti, *Diabetes*, 2004, **53**, 1261.
11 K. G. M. Alberti, P. Zimmet and J. Shaw, *Lancet*, 2005, **366**, 1059.
12 W. M. U. Daniels, S. J. van Rensburg, J. M. van Zyl and J. J. F. Taljaard, *J. Pineal Res.*, 1998, **24**, 78.
13 (*a*) A. J. Bruce-Keller, J. G. Begley, W. Fu, D. A. Butterfield, D. E. Bredesen, J. B. Hutchins, K. Hensley and M. P. Mattson, *J. Neurochem.*, 1998, **70**, 31; (*b*) R. J. Mark, K. S. Fuson and P. C. May, *J. Neurochem.*, 1999, **72**, 1146.
14 E. Herker and M. Ott, *Trends Endocrinol. Metab.*, 2011, **22**, 241.
15 (*a*) R. Munir, H. Usman, S. Hasnain, K. Smans, H. Kalbacher and N. Zaidi, *Biochimie*, 2014, **102**, 9; (*b*) C. R. Santos and A. Schulze, *FEBS J.*, 2012, **279**, 2610.
16 S. M. Borisov and O. S. Wolfbeis, *Chem. Rev.*, 2008, **108**, 423.
17 P. Greenspan, E. P. Mayer and S. D. Fowler, *J. Cell Biol.*, 1985, **100**, 965.
18 Y. Ohsaki, Y. Shinohara, M. Suzuki and T. Fujimoto, *Histochem. Cell Biol.*, 2010, **133**, 477.
19 P. M. Gocze and D. A. Freeman, *Cytometry*, 1994, **17**, 151.
20 A. Loudet and K. Burgess, *Chem. Rev.*, 2007, **107**, 4891.
21 K. Yen, T. T. Le, A. Bansal, S. D. Narasimhan, J.-X. Cheng and H. A. Tissenbaum, *PLoS One*, 2010, **5**, e12810.
22 T. Förster and K. Kasper, *Z. Phys. Chem.*, 1954, **1**, 275.
23 C. W. Leung, Y. Hong, S. Chen, E. Zhao, J. W. Lam and B. Z. Tang, *J. Am. Chem. Soc.*, 2013, **135**, 62.
24 (*a*) Y. Hong, J. W. Lam and B. Z. Tang, *Chem. Commun.*, 2009, 4332; (*b*) Y. Hong, J. W. Lam and B. Z. Tang, *Chem. Soc. Rev.*, 2011, **40**, 5361; (*c*) Y. Yuan, G. Feng, W. Qin, B. Z. Tang and B. Liu, *Chem. Commun.*, 2014, **50**, 8757.
25 J. Luo, Z. Xie, J. W. Y. Lam, L. Cheng, B. Z. Tang, H. Chen, C. Qiu, H. S. Kwok, X. Zhan, Y. Liu and D. Zhu, *Chem. Commun.*, 2001, 1740.
26 J. Mei, Y. Hong, J. W. Lam, A. Qin, Y. Tang and B. Z. Tang, *Adv. Mater.*, 2014, **26**, 5429.
27 (*a*) F. Hu, Y. Huang, G. Zhang, R. Zhao, H. Yang and D. Zhang, *Anal. Chem.*, 2014, **86**, 7987; (*b*) C. C. Chang, M. C. Hsieh, J. C. Lin and T. C. Chang, *Biomaterials*, 2012, **33**, 897; (*c*) M.-C. Hsieh, C.-H. Chien, C.-C. Chang and T.-C. Chang, *J. Mater. Chem. B*, 2013, **1**, 2350.
28 (*a*) W.-C. Wu, C.-Y. Chen, Y. Tian, S.-H. Jang, Y. Hong, Y. Liu, R. Hu, B. Z. Tang, Y.-T. Lee, C.-T. Chen, W.-C. Chen and A. K. Y. Jen, *Adv. Funct. Mater.*, 2010, **20**, 1413; (*b*) Q. Hu, M. Gao, G. Feng and B. Liu, *Angew. Chem., Int. Ed.*, 2014, **53**, 14225; (*c*) M. Gao, C. K. Sim, C. W. Leung, Q. Hu, G. Feng, F. Xu, B. Z. Tang and B. Liu, *Chem. Commun.*, 2014, **50**, 8312.
29 (*a*) Y. Chen, L. Qiao, B. Yu, G. Li, C. Liu, L. Ji and H. Chao, *Chem. Commun.*, 2013, **49**, 11095; (*b*) W. D. Chen, D. W. Zhang, W. T. Gong, Y. Lin and G. L. Ning, *Spectrochim. Acta, Part A*, 2013, **110**, 471.
30 (*a*) D. Ding, J. Liu, G. Feng, K. Li, Y. Hu and B. Liu, *Small*, 2013, **9**, 3093; (*b*) W. Qin, D. Ding, J. Liu, W. Z. Yuan, Y. Hu, B. Liu and B. Z. Tang, *Adv. Funct. Mater.*, 2012, **22**, 771.
31 (*a*) R. T. Kwok, C. W. Leung, J. W. Lam and B. Z. Tang, *Chem. Soc. Rev.*, 2015, **44**, 4228; (*b*) D. Ding, K. Li, B. Liu and B. Z. Tang, *Acc. Chem. Res.*, 2013, **46**, 2441; (*c*) J. Geng, K. Li, W. Qin, B. Z. Tang and B. Liu, *Part. Part. Syst. Charact.*, 2014, **31**, 1238.
32 E. Wang, E. Zhao, Y. Hong, J. W. Y. Lam and B. Z. Tang, *J. Mater. Chem. B*, 2014, **2**, 2013.
33 (*a*) W. Rettig, *J. Phys. Chem.*, 1982, **86**, 1970; (*b*) M. Koenig, T. Torres, V. Barone, G. Brancato, D. M. Guldi and G. Bottari, *Chem. Commun.*, 2014, **50**, 12955; (*c*) Z. R. Grabowski, K. Rotkiewicz and W. Rettig, *Chem. Rev.*, 2003, **103**, 3899.

